

WELCOME TO THE NEWSLETTER e-SCIENCE PUTRA. THIS ISSUE PRESENT RESEARCH ACTIVITIES FROM JANUARY TO APRIL 2022 WHICH HIGHLIGHTS THE LATEST RESEARCH FINDINGS AND ACTIVITIES BY THE FACULTY MEMBERS. WE'RE HAPPY TO SHARE OUR NEWSLETTER WITH COMMUNITY, ALUMNI, AND FRIENDS.

eISSN 2805-4512



HIGHLIGHTS

- Nanocomposites for supercapacitors
- Unmanned Aerial Vehicles (UAV)
- Price Path Simulation
- Feeding and Trophodynamics of a Tropical Jellyfish
- Fractional Differential Equations with Caputo derivative

LAYER-BY-LAYER NANOCOMPOSITES FOR SUPERCAPACITORS



Report by: Assoc. Prof. Dr. Yusran Sulaiman
Expertise: Analytical Chemistry, Electrochemistry, Materials Chemistry
Department of Chemistry, Faculty of Science, Universiti Putra Malaysia
Email: yusran@upm.edu.my

In recent years, the demand for reliable, efficient, sustainable and high-powered energy storage devices for vehicles and mobile electronic devices has increased dramatically. Batteries as a conventional charge storage device have the drawback of relatively slow charging/discharging rates and short cycle life. These problems can be overcome by supercapacitors as it can provide a large amount of energy, fast charging/discharging rates, high power density and longer life cycle compared to batteries. The energy storage performance is strongly depending on the properties of an electrode material such as the active surface area of electrode and electrode structure architecture, and the presence of active components into the electrode.

Therefore, we have constructed multilayer films through a layer-by-layer approach, which is easy and straightforward procedure for modifying electrode materials. Various nanocomposites have been used to develop supercapacitor devices such as conducting polymers, carbon-based materials, layered-double hydroxides, etc. utilising this approach. Findings from this work have been published in highly reputed journals [1-3]. This work has also been filed a patent (PI2018702018) and has received 2-prestigious awards in International Invention, Innovation & Technology Exhibition (ITEX) and International Conference and Exposition on Inventions by Institutions of Higher Learning (PECIPTA).



Figure 2: Assoc. Prof. Dr. Yusran Sulaiman and his student, Dr. Shalini Kulandaivalu during the exhibition.

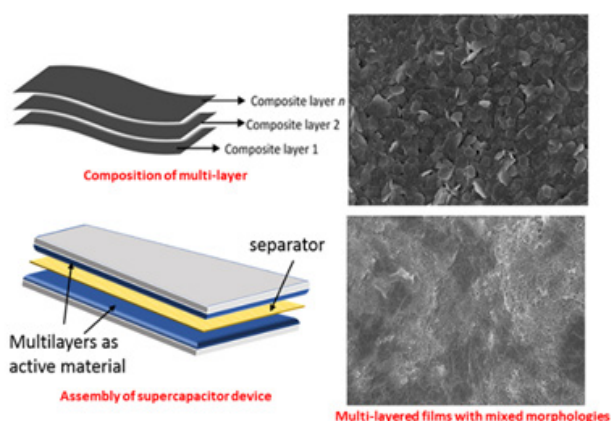


Figure 1: Composition of multi-layer films, assembly of supercapacitor device and morphology of multi-layer films.

References

- Shalini Kulandaivalu and Yusran Sulaiman (2020) *Journal of Materials Science: Materials in Electronics*. 31 (6). 4882-4894.
- Shalini Kulandaivalu, Muhammad Naim Mohd Azahari, Nur Hawa Nabilah Azman and Yusran Sulaiman (2020) *Journal of Energy Storage*. 28.101219
- Shalini Kulandaivalu, Mohd Zobir Hussein, Adila Mohamad Jaafar, Muhammad Amirul Aizat Mohd Abdah, Nur Hawa Nabilah Azman and Yusran Sulaiman (2019). *RSC Advances*. 9. 40478 – 40486.

UNMANNED AERIAL VEHICLES (UAV): AN APPROACH FOR SEAGRASS HABITAT ASSESSMENT



Report by: Professor Dr. Japar Sidik Bujang,
Expertise: Aquatic Biology (Mangrove and Seagrasses)
Department of Biology, Faculty of Science, Universiti Putra Malaysia
e-mail: japar@upm.edu.my

Project Member:
Prof. Dr. Muta Harah Zakaria
Department of Aquaculture, Faculty of Agriculture, Universiti Putra Malaysia

Habitat assessment, be it a forest on land or submerged seagrass or benthic communities such as seaweeds, has been studied by employing various methods and yielding results at different resolutions. Examples of such methods are (a) Satellite remote sensing, e.g., the effect of reclamation activities on seagrass meadow (Hossain et al. 2019), documented changes at a broad scale with limitations to resolution depending on the satellite images. Ground surveys or ground truth are undoubtedly needed, allowing image data related to actual features on the ground. The collection of ground-truth data enables calibration of remote-sensing data and aids in the interpretation and analysis of what is being sensed, (b) ground surveys or ground-truth and permanent transect-quadrat methods (Fortes, 2011), documented good changes in vegetation cover and plant species at a much smaller scale and hypothetically assumed as the representative of the whole area of seagrass or seaweed. Based on the literature search, scientists are looking into the feasibility of unmanned aerial vehicles (UAV) for conducting an ecological survey: surveying marine fauna: a dugong case study has yielded promising results, readily identifying dugongs within the images, cost-effective than dugong sightings surveys using manned aircraft.

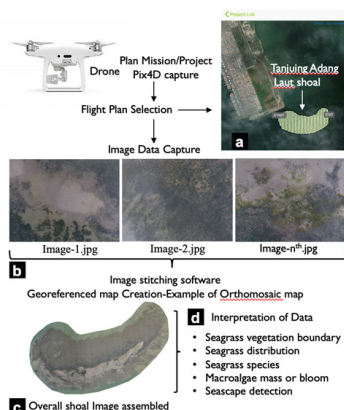


Figure 1: Mapping of the seagrass shoal (a) Planned flight path, (b) Examples of images acquired by DJI drone Phantom 4 Pro V2, (c) An example of orthomosaic of an 11.2 ha Tanjung Adang Laut shoal created in photogrammetry software and (d) Data obtained from the high-resolution Orthomosaic map.

We also use UAV while conducting seagrass ecological assessment at Tanjung Adang Laut shoal, near the Port of Tanjung Pelepas, Gelang Patah, Johor. We use a DJI Phantom 4 Pro V2 drone, autonomous (without recourse to our remote controller), following a predetermined Flight Plan at a specified height (set at 30 m, drone flying at fast speed in Pix4D software, Figure 1a), capturing geotagged images with front and side image overlap of 55% at the planned Flight Plan. While the drone is capturing the geotagged images, we, the researchers, are conducting our ground-truth, laying line transect and quadrats, photo capturing, and recording plant species and cover. The capture of geotagged images and our ground-truthing is conducted in real-time and space. Images captured (in our case, 1410 images, Figure 1b) by the drone are assembled using photogrammetry

software, e.g., Pix4Dmapper or DroneDeploy, or Microsoft Image composite editor, to produce a high-resolution orthomosaic of the seagrass meadow (Figure 1c, map of the shoal of Tanjung Adang Laut). The orthomosaic from the in-situ mapping provides valuable information. Information from the map (Figure 1d) is real-time data and combined with the ground surveys data, provided the tools for the interpretation of orthomosaic map: (a) Seagrass vegetation boundary, (b) Seagrass or any other plant, e.g., macroalgae (seaweed) distribution, (c) Seagrass or macroalgae mass or bloom and (d) Seascapes detection other than seagrass or macroalgae. Figure 2. (a)-(d) show the details of seascape features of Tanjung Adang Laut, Gelang Patah, southwest Johor, seagrass habitat map,

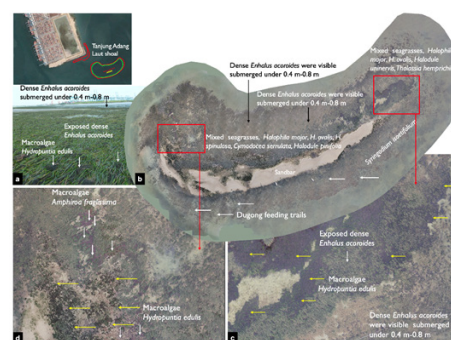


Figure 2: Tanjung Adang Laut shoal, Gelang Patah, southwest Johor. Dated 30 April 2021. The real-time orthomosaic map detailing the various seascapes. (a) Seagrass meadow with the dominant *Enhalus acoroides* exposed or submerged at low tide from -0.4 to -0.8 m. (b) Aerial high-resolution orthomosaic map showing 11.3 ha seagrass meadow with clear *Enhalus acoroides* boundary. The Sandbar is a unique structure, dynamic, and the area of accreted sediment. *Halophila ovalis*/H. major and *Halodule uninervis*, growing and expanding their rhizomes on the Sandbar. Dugong feeding trails (white arrows) over *Halophila* patches were detected in April 2021. (c) Masses of macroalgae, *Hydropuntia edulis* (dark color, yellow arrows) covering the *Enhalus acoroides* and other seagrasses and (d) Masses of macroalgae, *Amphiroa fragilissima* (reddish, white arrows), and *Hydropuntia edulis* (dark color, yellow arrows) among seagrasses.

Photo credit: Japar Sidik B. & Muta Harah Z. © Rights remain with the authors.

References

- Hossain, M.S., Hashim, M., Bujang, J.S., Zakaria, M.H., Aidy, M.M. (2019). Assessment of the impact of coastal reclamation activities on seagrass meadows in Sungai Pulai estuary, Malaysia, using Landsat data (1994–2017). *International Journal of Remote Sensing* 40(9):3571–3605. <https://doi.org/10.1080/01431161.2018.1547931>
- Fortes, E.T.G. (2011). Methods of seagrass-seaweed community using the line transect-quadrat method. In: Ogawa, H., Japar Sidik, B. & Muta Harah, Z. (eds.). *Seagrasses: Resource status and trends in Indonesia, Japan, Malaysia, Thailand and Vietnam*. Pp. 153–162. Japan Society for The Promotion of Science (JSPS) and Atmosphere and Ocean Research Institute (AORI), The University of Tokyo. Seizando-Shoten Publishing Co., Ltd., Tokyo, Japan. Hodgson, A., Kelly, N., Peel, D. (2013.). *Unmanned Aerial Vehicles (UAVs) for surveying marine fauna: a dugong case study*. *PLoS One* 8(11): e79556. <https://doi.org/10.1371/journal.pone.0079556>

PRICE PATH SIMULATION WITH GEOMETRIC BROWNIAN MOTION AND GEOMETRIC FRACTIONAL BROWNIAN MOTION MODELS



Report by: Assoc. Prof. Dr. Siti Nur Iqmal Ibrahim,

Expertise: Financial Mathematics

Department of Mathematics and Statistics, Faculty of Science, Universiti Putra Malaysia

e-mail: iqmal@upm.edu.my

Many prediction models have been developed and improved to assist investors in making investment decision by providing an overlook of the price paths, hence minimum investment risk. The geometric fractional Brownian motion (gfBm) model improves the accuracy of the price modelling by incorporating the Hurst exponent into the price dynamics, which provides information on the self-similarity level in each time series, therefore able to explain more behaviours of price changes.

The price S_t follows a geometric Brownian motion (gBm) when it follows the dynamics

$$dS_t = \mu S_t dt + \sigma S_t dW_t$$

where W_t^H is a Brownian motion, and the solution is

$$S_t = S_0 e^{\left(\mu t - \frac{1}{2}\sigma^2 t + \sigma W_t\right)}$$

The gfBm is more general than the gBm, where the price follows the dynamics

$$dS_t = \mu S_t dt + \sigma S_t dW_t^H$$

where W_t^H is an fBm with

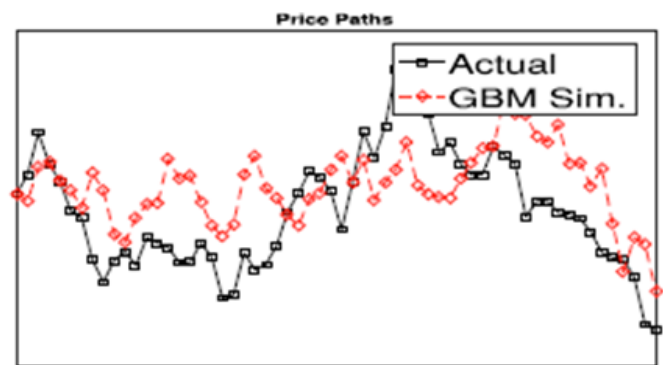
$$H \in (0,1)$$

and the solution is

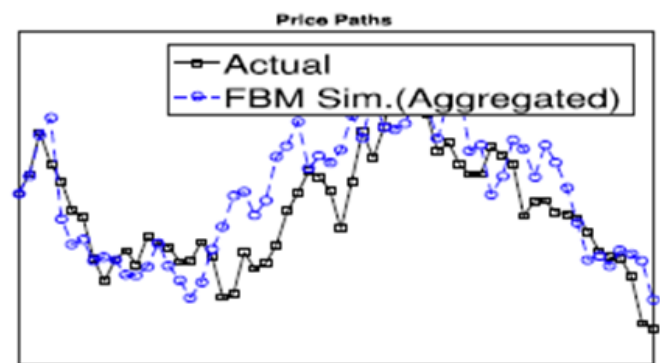
$$S_t = S_0 e^{\left(\mu t - \frac{1}{2}\sigma^2 t^{2H} + \sigma W_t^H\right)}$$

Both processes have constant drift μ and constant volatility σ .

This study applies the gBm and gfBm models to simulate price paths of Malaysian crude palm oil, and tests both models for accuracy of the simulations by comparing with the actual prices, using the mean absolute percentage error (MAPE) taken relative to the simulated prices. For instance, for a 5-year period simulation, the MAPE using GBM is 10.9386, while the MAPE using GFBM is 7.6137. This shows higher accuracy in the simulation by the GFBM model.



5-year price path simulation using gBm



5-year price path simulation using gfBm

ASSESSING THE FEEDING AND TROPHODYNAMICS OF A TROPICAL JELLYFISH COMMUNITY



Report by: Dr. Wan Mohd Syazwan Wan Solahudin,
Expertise: Marine Ecology
Department of Biology, Faculty of Science, Universiti Putra Malaysia
e-mail: mhdasyazwan@upm.edu.my

Massive and seasonal population blooms of jellyfish (Phylum Cnidaria, Class Scyphozoa) in worldwide oceans have resulted in the disruption of marine ecosystems and associated coastal communities. Jellyfish blooms could directly affect fishing operations by damaging fishing gears and indirectly impact local fishery stocks via intraguild competition, predation impacts, and redirecting energy flows in food webs. Conversely, the blooms may provide economic benefits to the jellyfish fishery (Syazwan et al., 2020). However, there is a lack of baseline ecological data regarding jellyfish in Malaysia or elsewhere in Southeast Asia, which could be used to mitigate the blooms' impacts and effectively manage the fast-growing jellyfish fishery. In view of this, a team of researchers from the Faculty of Science, UPM and the Institute of Ocean and Earth Sciences, UM has instigated a collaborative effort to investigate the feeding ecology of local jellyfish species in the Klang Strait, an area of fishery importance where jellyfish bloom events are on the rise. The study is the first to use the dual approach of stomach content examination and stable isotope analysis to investigate the diet, trophic position and the relative contribution of primary producers to the nutrition of jellyfish in shallow tropical waters (Syazwan et al., 2021).

Dietary analyses showed that jellyfish species in the Klang Strait primarily feed on zooplankton with significant reliance on copepods as prey. They can be classified into three major feeding guilds, namely specialized copepod feeders (*Phyllorhiza punctata*, *Rhopilema esculentum*, *Lychnorhiza malayensis*, *Rhopilema hispidum*), copepod and macrozooplankton feeders (*Cyanea* sp.) and mixed feeders (*Lobonemoides robustus*). Stable isotopic mixing models further revealed that jellyfish rely heavily on benthic and pelagic primary sources through the predation of zooplankton. Jellyfish thus plays a significant role in coupling the benthic and pelagic primary production to human or other predators, and as an important carbon exporter from nearshore to neritic and offshore waters (Figure 1). It was evident that high in situ productions and food resources in the mangrove and mudflat habitats allow them to serve as substantial feeding and nursery grounds for tropical jellyfish species, thus providing the ideal condition for jellyfish populations to bloom. Given the importance of jellyfish as zooplankton predator and potential competitor for zooplanktivorous fishes and invertebrates, further study to elucidate trophic interactions among these marine biotas in the Klang Strait is urgently needed.

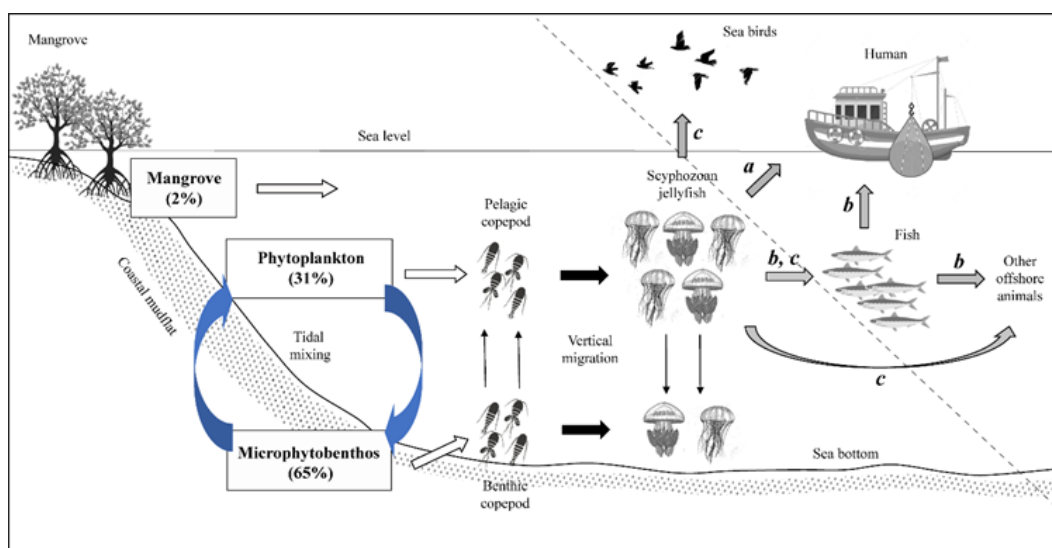


Figure 1: Schematic diagram (not to scale) of the relationships between primary producers (mangrove, microphytobenthos and phytoplankton), major zooplankton prey (copepod), scyphozoan jellyfishes and other top predators in the Klang Strait. Blue arrows indicate the tidal mixing of phytoplankton and microphytobenthos. White arrows indicate inputs of major (microphytobenthos and phytoplankton) and minor (mangrove) primary sources for scyphozoan jellyfish, while black arrows indicate trophic links from primary consumers to jellyfish based on the present study (left side of dotted oblique line). Grey arrows indicate hypothetical trophic links from jellyfish to higher level consumers based on other works conducted in the Klang Strait (a, b) and other regions (c). Thin line arrows indicate vertical migration by scyphozoan jellyfishes and their copepod prey. Percentage indicates overall proportion contribution of each primary source to scyphozoan jellyfish based on MixSIAR results. The slope of the coastal mudflat from the mangrove forest is gentle but exaggerated here for clarity.

References

Syazwan, W. M., Rizman-Idid, M., Low, L. B., Then, A. Y. H., & Chong, V. C. (2020a). Assessment of scyphozoan diversity, distribution and blooms: Implications of jellyfish outbreaks to the environment and human welfare in Malaysia. *Regional Studies in Marine Science*, 39(2020), 101444. DOI: 10.1016/j.rsma.2020.101444

Syazwan, W. M., Then, A. Y. H., & Chong, V. C. (2021). Trophic ecology of a tropical scyphozoan community in coastal waters: Insights from stomach content and stable isotope analyses. *Continental Shelf Research*, 225(2021), 104481. <https://doi.org/10.1016/j.csr.2021.104481>

NUMERICAL SOLUTIONS OF FRACTIONAL DIFFERENTIAL EQUATIONS WITH CAPUTO DERIVATIVE



Report by: Prof. Dr. Zanariah Abdul Majid,
Expertise: Numerical Analysis
Department of Mathematics and Statistics, Faculty of Science, Universiti Putra Malaysia
e-mail: am_zana@upm.edu.my

Fractional differential equations have recently proven to be useful in a wide range of domains, including medicine, applied sciences, and engineering. The main objective of this study is to propose an Adams-type multistep method (FAM22) for fractional order differential equations. The method is developed by combining the Lagrange interpolation with the concept of the Adams–Moulton method for fractional case. In this study, the fractional derivative is in the Caputo derivative operator. The analysis of the proposed method is presented in terms of order of the method, order of accuracy, and convergence analysis, with the proposed method being proved to converge (Zabidi et al. (2022)). The stability of the method is also examined, where the stability regions appear to be symmetric to the real axis for various values of α . In order to validate the competency of the proposed method, several numerical examples for solving linear and nonlinear fractional differential equations have been tested. The proposed method will be presented in the numerical predict–correct technique for the condition where $\alpha \in (0,1)$, in which α represents the order of fractional derivatives of $D^\alpha y(t)$.

Foremost, it is given that the fractional initial value problem (FIVP) is said to be in the form of

$${}_C D_{t_0}^\alpha y(t) = f(t, y(t)), \quad y(t_0) = y_0,$$

where α is the fractional order and ${}_C D_{t_0}^\alpha$ indicates the fractional Caputo's α -derivative operator.

The developed formula of the implicit part in FAM22 is as follows:

$$y(t_{i+1}) = y(t_i) + \frac{h^\alpha}{\Gamma(\alpha)} \left[\left(\frac{(i+1)^\alpha}{\alpha} + \frac{(i)^{\alpha+1} - (i+1)^{\alpha+1}}{\alpha+1} \right) F_{i+1} + \left(\frac{-(i)^\alpha}{\alpha} + \frac{(i+1)^{\alpha+1} - (i)^{\alpha+1}}{\alpha+1} \right) F_i \right].$$

The formula is the corrector formula of the FAM22.

Numerical Example

Example 1:

FIVP with variable coefficients.

$$D^\alpha y(t) = \frac{40320}{\Gamma(9-\alpha)} t^{8-\alpha} - 3 \frac{\Gamma(5+\frac{\alpha}{2})}{\Gamma(5-\frac{\alpha}{2})} t^{4-\frac{\alpha}{2}} + \frac{9}{4} \Gamma(\alpha+1), \quad y(0) = 0$$

The exact solution is

$$y(t) = t^8 - 3t^{4+\frac{\alpha}{2}} + \frac{9}{4} t^\alpha$$

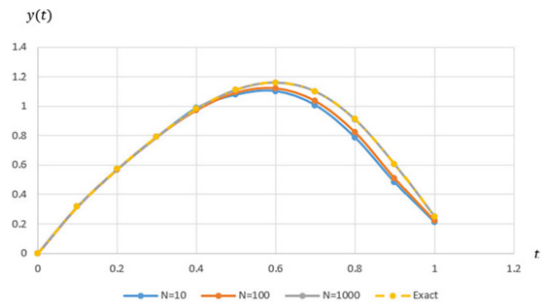


Figure 1: Graph of approximate solution $y(t)$ against t as $\alpha = 0.50$ for solving Example 1 using FAM22.

Figure 1 displays the performance graph of approximate solutions for $N = 10, 100, 1000$ and $\alpha = 0.50$ when solving Example 1. The graph indicates that as the number of intervals for each point N increases, the approximate solutions approach the exact solution.

Example 2:

An application problem of fractional Riccati differential equation (FRDE):

$$D^\alpha y(t) = -y^2(t) + 1, \quad y(0) = 0.$$

The exact solution is

$$y(t) = \frac{e^{2t}-1}{e^{2t}+1} \text{ as } \alpha = 1.0.$$

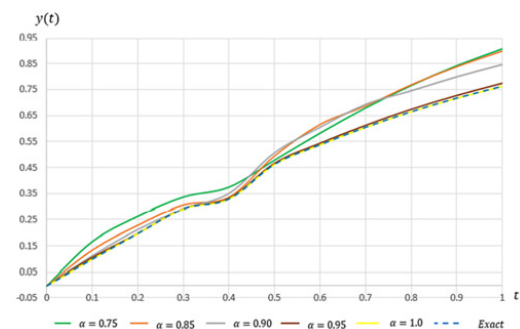


Figure 2: Graph of approximate solution $y(t)$ against t as $N=10$ for solving Example 2 using FAM22.

For better analysis, the graph for solving the FRDE problem (Example 2) using FAM22 is visualized in Fig. 2 for $N = 10$ when $\alpha = 0.75, 0.85, 0.90, 0.95, 1.0$. The graph shows as α increases, the approximate solutions $y(t)$ approaches the exact solution. The outcome for an increment in the order of FDE, α is also investigated where, as α increases and approaches 1.0, the results yield better accuracy. In addition, the approximate solutions indeed converge as the step size h decreases.

Reference

Zabidi, N.A., Majid, Z.A., Kilicman, A. Numerical solution of fractional differential equations with Caputo derivative by using numerical fractional predict–correct technique. *Adv Cont Discr Mod* 2022, 26 (2022). <https://doi.org/10.1186/s13662-022-03697-6>

**Science is much more than just a body of KNOWLEDGE.
It is a way of THINKING.**

EDITORIAL TEAM:

Prof. Dr. Zanariah Abdul Majid
Assoc. Prof. Dr. Mohammad Noor Amal Azmai
Dr. Mohd Hafiz Mohd Zaid
Jivananthan a/l Arumugam
Ruzila Hussain Shaari
Farah Syakila Mohd Raziff

FACULTY OF SCIENCE, UNIVERSITI PUTRA MALAYSIA, 43400 UPM SERDANG, SELANGOR DARUL EHSAN, MALAYSIA

☎ +603 97696601/6602/6603 🌐 www.science.upm.edu.my ✉ fs_tdps@upm.edu.my